Supporting Information

for

A robust electrocatalytic activity toward hydrogen evolution reaction from W/W_2C heterostructured nanoparticles coated by N,P dual-doped carbon layer

Quan Zhang[a#], Fang Luo[a#], Hao Hu[a], Ruizhi Xu[a], Konggang Qu[b], Zehui Yang[a*], Jingxiang Xu[c*] and Weiwei Cai[a*]

[a]Sustainable Energy Laboratory, Faculty of Materials Science and Chemistry, China University of Geosciences Wuhan, 388 Lumo RD, Wuhan, 430074, China

[b]Shandong Provincial Key Laboratory/Collaborative Innovation Center of Chemical Energy Storage & Novel Cell Technology, Liaocheng University, Liaocheng, 252059, China.

[c]College of Engineering Science and Technology, Shanghai Ocean University, Shanghai 201306, China

Experimental section

Materials: Phosphotungstic acid ($H_3PW_{12}O_{40}$ ·xH2O) was purchased from Aladdin. Aniline, ammonium persulfate (APS) and sulfuric acid (H_2SO_4, 98%) were obtained from Sinopharm Chemical Reagent Co. Ltd. Commercial Pt/C (Pt: 20 wt%) and Nafion aqueous solution (5 wt%) were provided by Alfa Aesar. All these chemicals were employed without any purification.

Synthesis of electrocatalyst: PANI/$H_3PW_{12}O_{40}$ hybrids were synthesized as follow: Briefly, 100 mg of $H_3PW_{12}O_{40}$ ·xH_2O was dispersed in 60 mL of 0.5 M H_2SO_4 solution and 42 μL of aniline monomer was added with strong stirring for 3 h in ice-water bath. Subsequently, 105 mg of APS was dissolved in 40 mL of 0.5 M H_2SO_4 solution with the mole ratio of 1:1 and was added to the mixture. The reaction process was conducted at low temperature (<5 ^oC) for 6 h. The product was filtered and washed with alcohol and Milli-Q water for several times, then dried for 12 h at 60 ^oC under vacuum to obtain power sample. Afterwards, the solid power products were annealed up to 900 ^oC in a tube furnace under a flow of Ar with different time. W@NPC, W/W_2C@NPC-1, W/W_2C@NPC-2 and W_2C@NPC were prepared with 1 h, 2 h, 3 h and 4 h, respectively.

Fundamental characterization: The powder X-ray diffraction (XRD) analysis was performed using Brucker AXS D8-Focus X-ray diffractometer with Cu-Ka radiation. The X-ray photoelectron spectroscopy (XPS) spectra measurements were carried out on Thermo-Scientific K-Alpha. The TEM images and various elemental distribution of electrocatalysts were observed by the means of a FEI Tecnai G2 F30 electron

microscope provided with an energy dispersive X-ray Spectroscope (Oxford INCA x-sight, England).

Electrochemical measurements: The electrochemical hydrogen evolution performance was performed on a typical three-electrode system using a Gamry interface 5000E instrument, where carbon rod and saturated calomel electrode act as counter and the reference electrode, respectively. 5 μL of homo-dispersed catalyst ink was pipetted on the glassy carbon with diameter of 3 mm used as the working electrode (catalyst mass loading: 0.283 mg cm^{-2}). LSV at a scan rate of 5 mV s^{-1} was conducted in N_2-saturated 0.5 M H_2SO_4 and 1 M KOH electrolyte. CV was employed between -0.2 and 0.2 V vs. RHE at 100 mV s^{-1}. The electrochemical double-layer capacitances were evaluated in the range from 0.16 to 0.26 V vs. RHE at different sweep rates from 10 to 100 mV s^{-1}. EIS was recorded in the frequency range from 1 MHz to 0.1 Hz at overpotential at 10 mA cm^{-2}. The amperometric (i-t) stability was measured at overpotential at 10 mA cm^{-2} for 10 h to illustrate the long-term stability. All the potentials were referenced to reversible hydrogen electrode.

Theoretical study: All periodic density functional theory (DFT) calculations with spin polarization were performed by using the Vienna ab initio simulation package (VASP) with the Perdew-Burke-Ernzerhof (PBE) exchange-correlation functional. The projector-augmented plane wave (PAW) was used to describe the interactions between core electrons and ions. A plane-wave cutoff energy was tested and set to 500 eV in all calculations. 3×3×1 Monkhorst-Pack grid k-points are employed for geometric optimization, and the convergence threshold is set as 10-4 eV in energy and

0.02 eV/Å in force, respectively. The W(110) slab model with 4 atomic layers and W_2C(-1-11) slab model with 21 atomic layers were employed, and the composited W/W_2C model was constructed by covering two W_2C layers on the W(110) slab. To investigate the effect of NPC on the HER activity, we constructed a W/W_2C@NPC model by covering the NPC layer on the W/W_2C slab. To minimize the lattice mismatch effect between the W/W_2C and NPC, a 2×2 supercell of W/W_2C slab was employed. To verify our calculation, the Pt(111) slab model with 4 atomic layers was also built (**Figure S1**). During the geometry optimization, the bottom two layers were kept fixed at the bulk positions while the atomic positions of other layers and adsorbates were relaxed. A vacuum distance of 15 Å was imposed between neighboring slab images in order to avoid interactions between periodic images. The hydrogen adsorption free energies were calculated by the following equation:

$$\Delta G_{H^*} = \Delta E_{H^*} + \Delta ZPE - T\Delta S,$$

where ΔE_{H^*} is the hydrogen chemisorption energy. ΔZPE and ΔS are the zero point energy difference and the entropy difference between the adsorbed and the gas phase, respectively. Here, the hydrogen chemisorption energy is defined by

$$\Delta E_{H^*} = 1/n\ (E(slab+nH) - E(Surf) - n/2\ E(H_2)),$$

where n is the number of H atoms in the calculations, *E(slab+nH)*, *E(Surf)*, and $E(H_2)$ are the total energies of the adsorption of n H atoms, clean surfaces, and gaseous hydrogen molecule, respectively. The above calculated values are shown in **Table S1**.

Table S1 The ΔE_{H^*}, ΔZPE, $T\Delta S$, ΔG_{H^*} values of the H* adsorbed on the surface of different models.

Models	ΔE_{H^*}/eV	ΔZPE/eV	$T\Delta S$/eV	ΔG_{H^*}/eV
W(110)	-0.818	0.035	-0.201	-0.581
W_2C(-1-11)	-0.576	-0.003	-0.198	-0.381
W/W_2C	-0.362	0.046	-0.207	-0.110
W/W_2C@NPC	-0.342	0.052	-0.219	-0.071
Pt(111)	-0.353	0.028	-0.221	-0.104

Table S2 Comparison of HER activities of reported W_xC based electrocatalysts.

Electrocatalyst	overpotential@10 mA cm^{-2} in 0.5 M H_2SO_4	overpotential@10 mA cm^{-2} in 1 M KOH	Ref.
W/W_2C@NPC	55 mV	82 mV	this work
Mo_2C-WC/NG	100 mV	93 mV	[1]
WC/NC	290 mV	300 mV	[2]
W_2C/WP@NC	83 mV	-	[3]
MoS_2/WC/RGO	200	-	[4]
W_2C@WC	310	-	[5]
$Mo_xW_{2-x}C$@C	127	106 mV	[6]
p-WC_x NWs	118	-	[7]
WxC/NG	77.82 mV	-	[8]
WC/G	120 mV	-	[9]
NC-NW	160 mV	-	[10]
Ni-WC	53 mV	77 mV	[11]

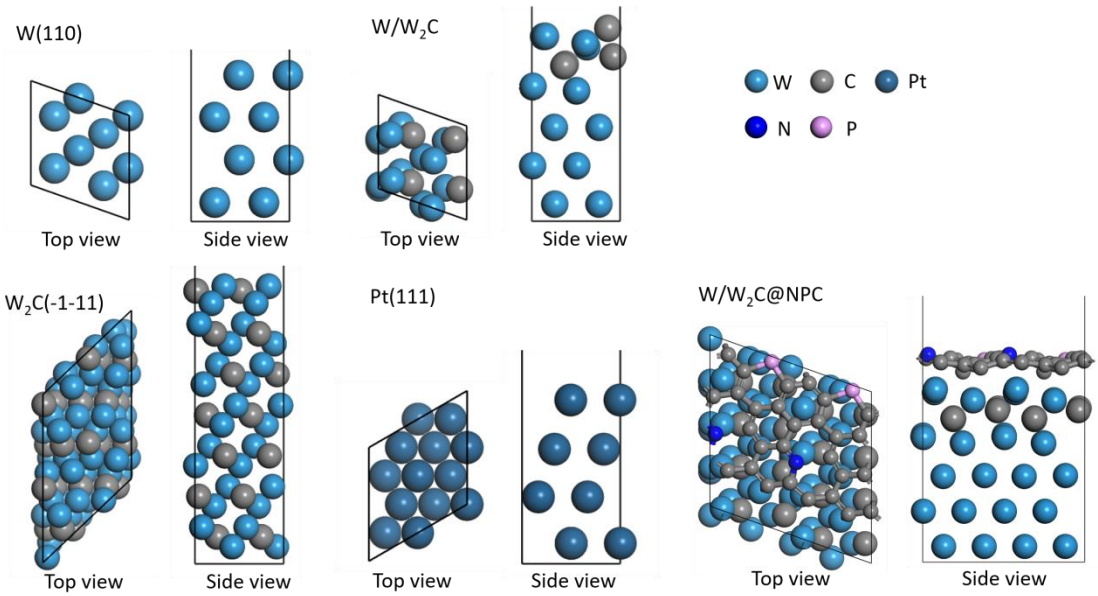

Figure S1 DFT calculated models of W(110), W_2C(-1-11), W/W_2C, Pt(111) and W/W2C@NPC.

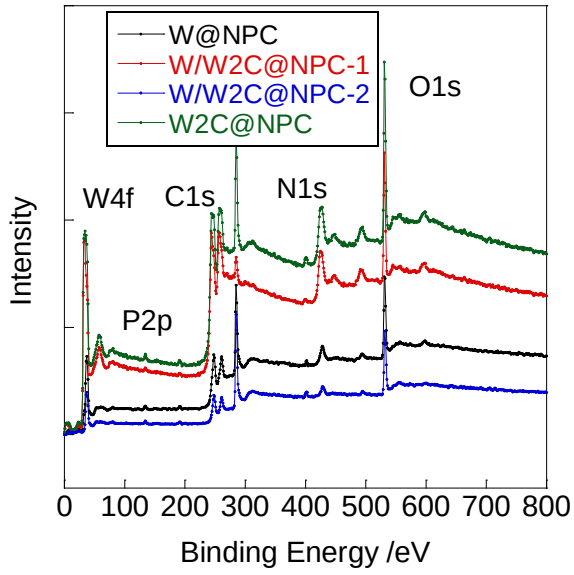

Figure S2 XPS survey scan of W@NPC, W_2C@NPC, W/W_2C@NPC-1 and W/W_2C@NPC-1 electrocatalysts.

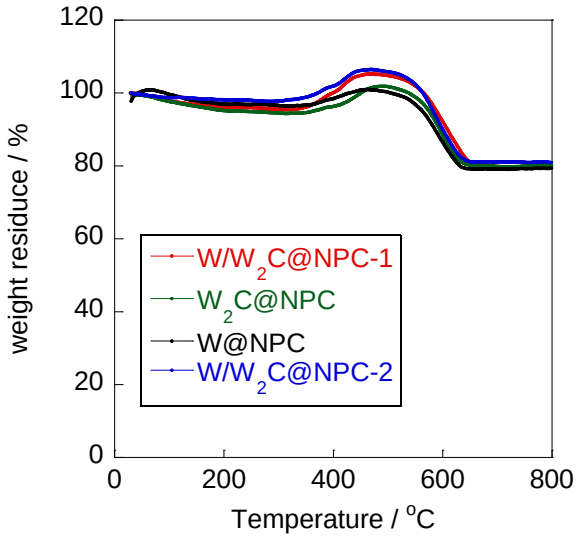

Figure S3 TGA curves of W@NPC, W_2C@NPC, W/W_2C@NPC-1 and W/W_2C@NPC-1 electrocatalysts measured from room temerpature to 800 °C with air flow.

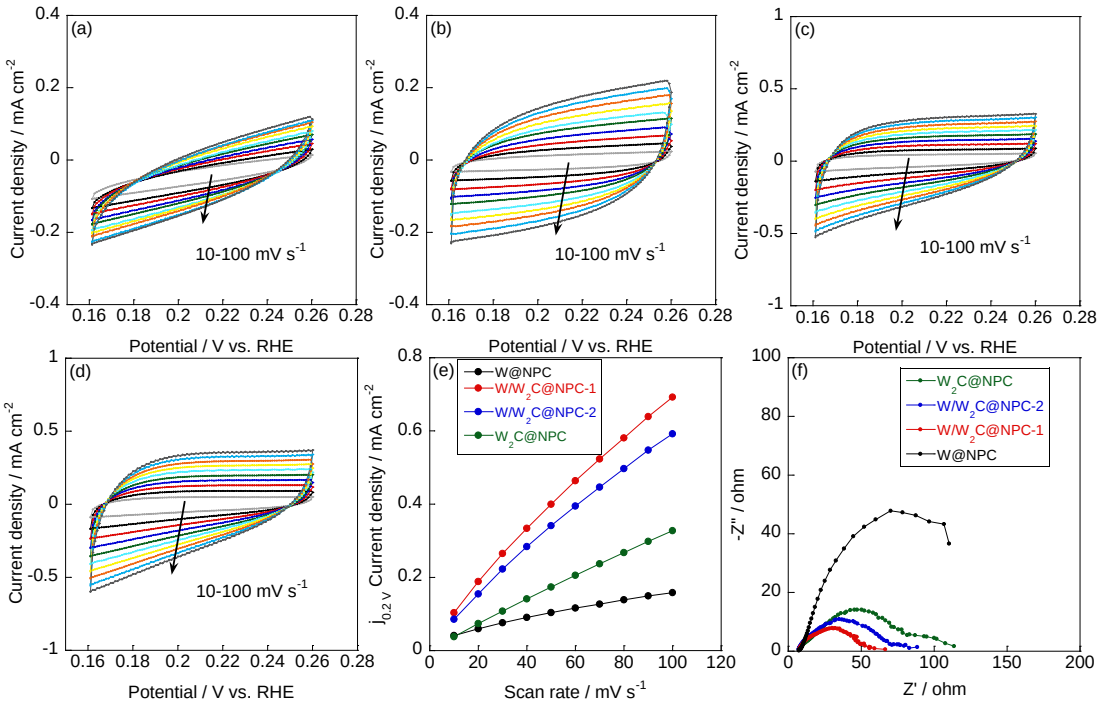

Figure S4 Cyclic voltammetry curves of W@NPC (a), W_2C@NPC (b), W/W_2C@NPC-1 (c) and W/W_2C@NPC-2 (d), respectively. ECSA (e) and EIS (f) of W@NPC, W_2C@NPC, W/W_2C@NPC-1 and W/W_2C@NPC-2.

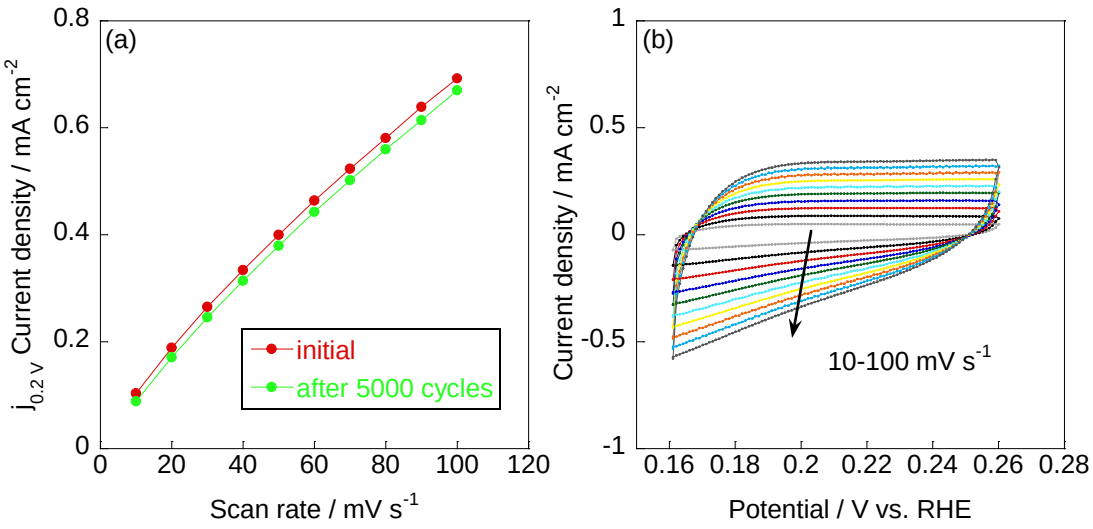

Figure S5 (a) Double layer capacitances of W/W_2C@NPC-1 before and after durability test in 0.5 M H_2SO_4 electrolyte. (b) Cyclic voltammetry curves of W/W_2C@NPC-1 after 5000 potential cycles.

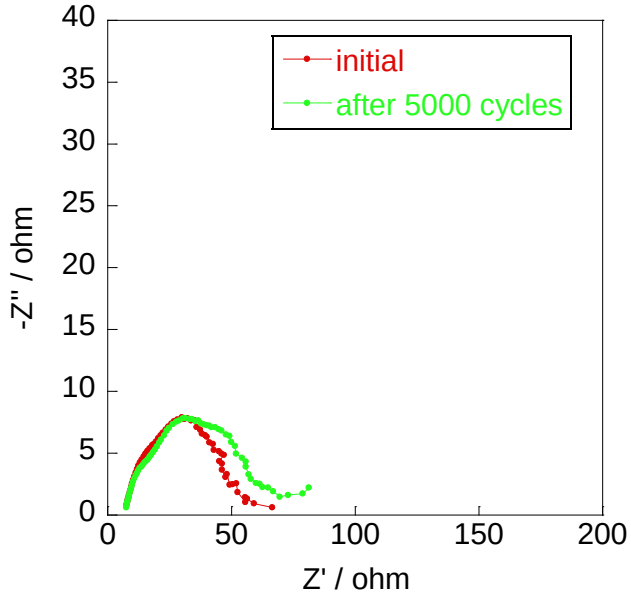

Figure S6 Electrochemical impedance spectroscopies (EIS) of W/W_2C@NPC-1 before and after durability test in 0.5 M H_2SO_4 electrolyte.

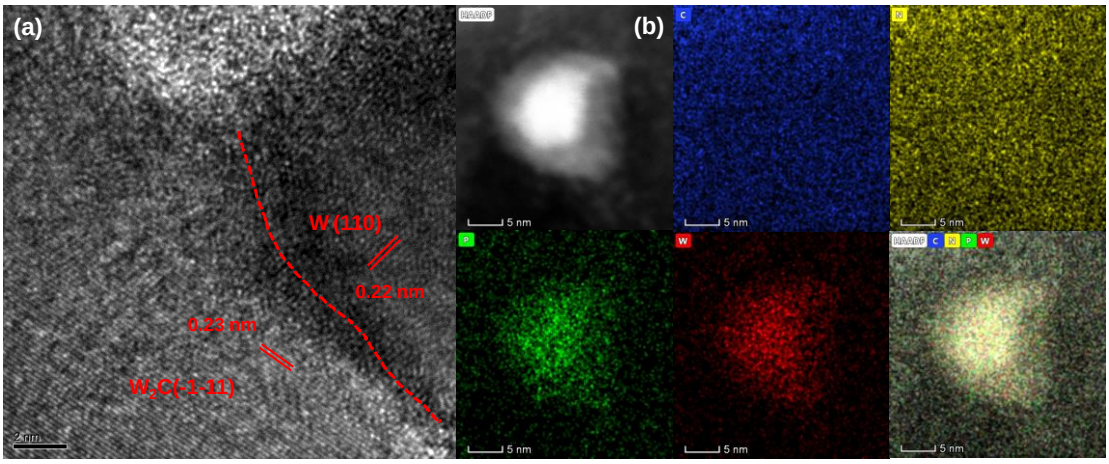

Figure S7 HR-TEM (a), HAADF-STEM (b) images and relative EDS mappings of W/W_2C@NPC-1 electrocatalyst after durability test in 0.5 M H_2SO_4 electrolyte.

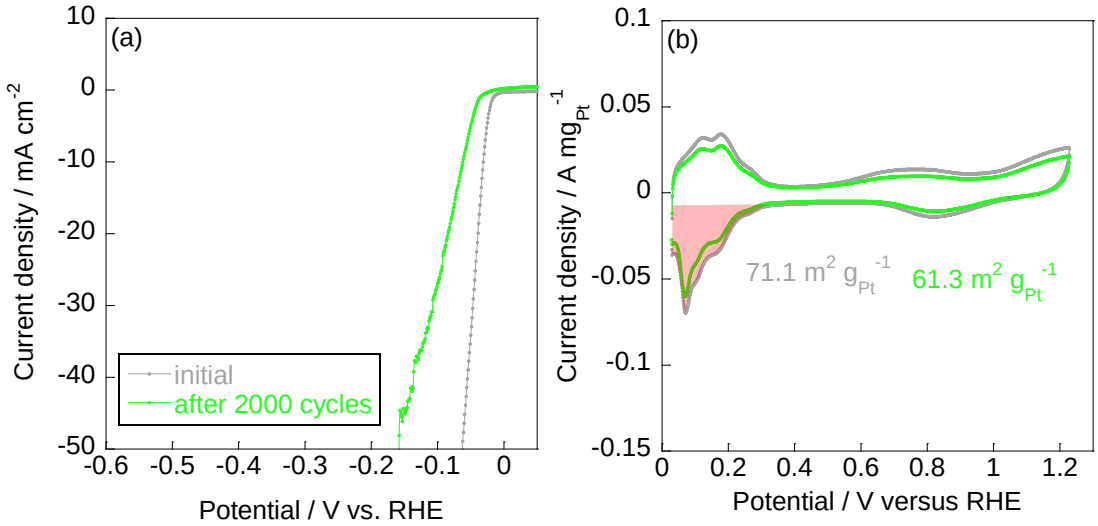

Figure S8 LSV curves (a) and CV curves (b) of commercial Pt/C electrocatalyst recorded before and after 2000 potential cycles in 0.5 M H_2SO_4 electrolyte.

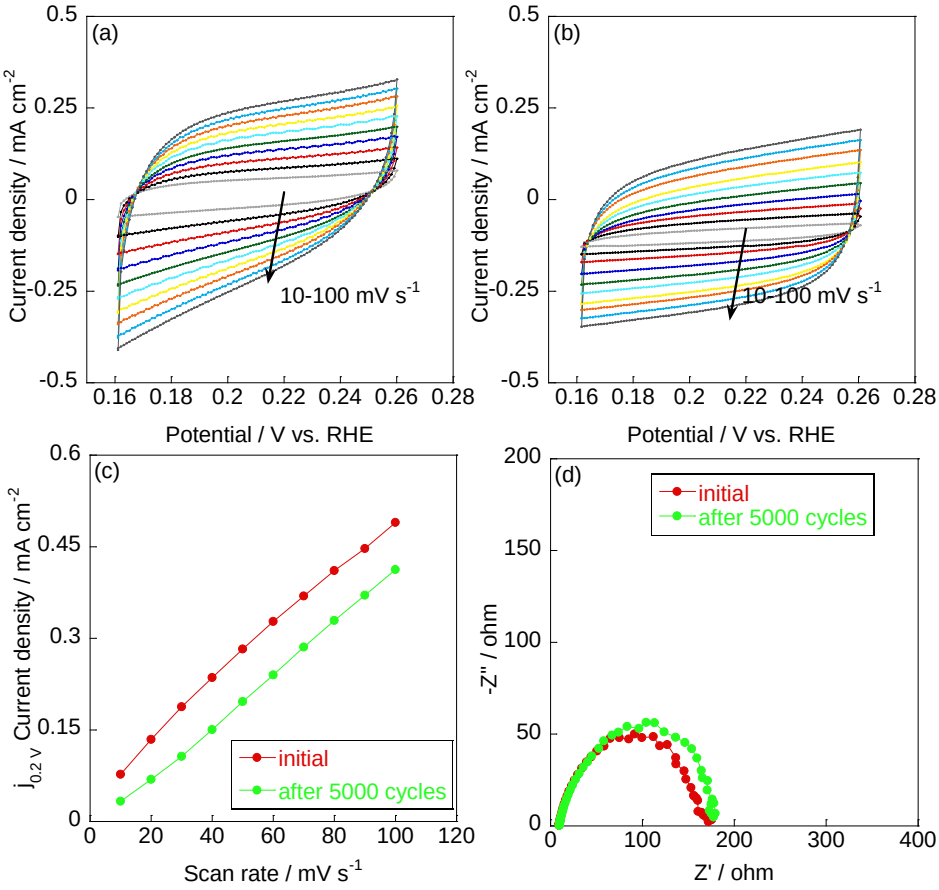

Figure S9 Cyclic voltammetry curves of W/W_2C@NPC-1 before (a) and after (b) durability test in 1 M KOH electrolyte. ECSA (c) and EIS (d) of W/W_2C@NPC-1 before and after durability test.

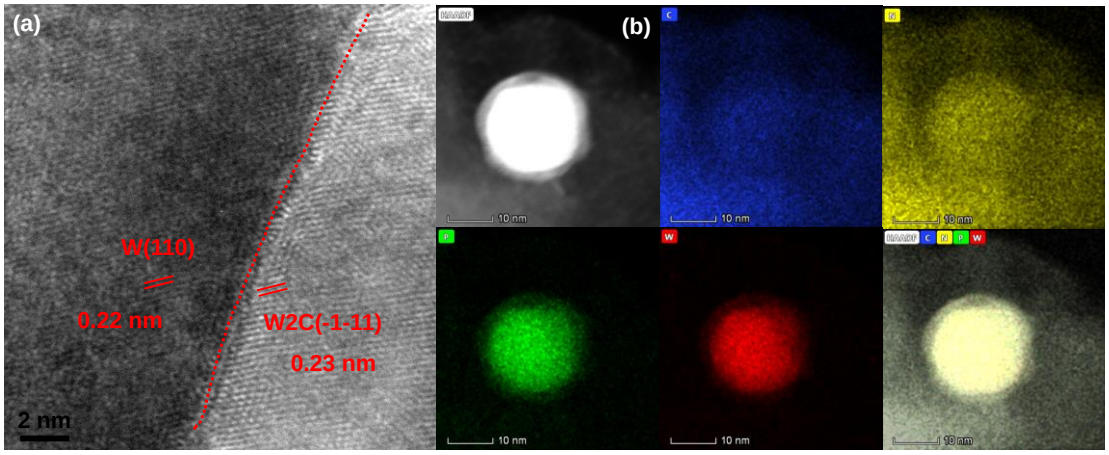

Figure S10 HR-TEM (a), HAADF-STEM (b) images and relative EDS mappings of W/W_2C@NPC-1 electrocatalyst after durability test in 1 M KOH electrolyte.

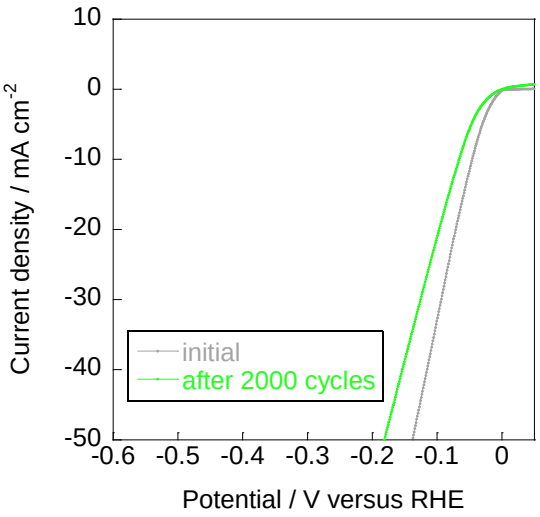

Figure S11 LSV curves of commercial Pt/C electrocatalyst recorded before and after 2000 potential cycles in 1 M KOH electrolyte.

References

1. L. Huo, B. Liu, Z. Gao and J. Zhang, *J. Mater. Chem. A*, 2017, **5**, 18494-18501.
2. L. Han, M. Xu, Y. Han, Y. Yu and S. Dong, *ChemSusChem*, 2016, **9**, 2784-2787.
3. M. Shi, W. Li, J. Fang, Z. Jiang, J. Gao, Z. Chen, F. Sun and Y. Xu, *Electrochim. Acta*, 2018, **283**, 834-841.
4. Y. Yan, B. Xia, X. Qi, H. Wang, R. Xu, J.-Y. Wang, H. Zhang and X. Wang, *Chem. Commun.*, 2013, **49**, 4884-4886.
5. S. Emin, C. Altinkaya, A. Semerci, H. Okuyucu, A. Yildiz and P. Stefanov, *Appl. Catal. B*, 2018, **236**, 147-153.
6. L. Lin, M. Chen and L. Wu, *Advanced Materials Interfaces*, 2018, **5**, 1801302.
7. B. Ren, D. Li, Q. Jin, H. Cui and C. Wang, *J. Mater. Chem. A*, 2017, **5**, 13196-13203.
8. J. Wang, W. Chen, X. Wang and E. Wang, *Electrochim. Acta*, 2017, **251**, 660-671.
9. M. Zeng, Y. Chen, J. Li, H. Xue, R. G. Mendes, J. Liu, T. Zhang, M. H. Rümmeli and L. Fu, *Nano Energy*, 2017, **33**, 356-362.
10. Y.-J. Ko, J.-M. Cho, I. Kim, D. S. Jeong, K.-S. Lee, J.-K. Park, Y.-J. Baik, H.-J. Choi and W.-S. Lee, *Appl. Catal. B*, 2017, **203**, 684-691.
11. Y.-Y. Ma, Z.-L. Lang, L.-K. Yan, Y.-H. Wang, H.-Q. Tan, K. Feng, Y.-J. Xia, J. Zhong, Y. Liu, Z.-H. Kang and Y.-G. Li, *Energy Environ. Sci.*, 2018, **11**, 2114-2123.